Received 00th January 20xx,
Accepted 00th January 20xx

DOI: 10.1039/x0xx00000x

From MAX phase carbides to nitrides: Synthesis of V_2GaC, V_2GaN and the carbonitride $V_2GaC_{1-x}N_x$

Niels Kubitza,[a] Andreas Reitz,[b] Anne-Marie Zieschang,[a] Hanna Pazniak,[c] Barbara Albert,[a] Curran Kalha,[d] Christoph Schlueter,[e] Anna Regoutz,[d] Ulf Wiedwald[c] and Christina S. Birkel [a,b]

[a.] *Eduard-Zintl-Institute, Technische Universität Darmstadt, Alarich-Weiss-Straße 12, 64287 Darmstadt, Germany*
[b.] *School of Molecular Sciences, Arizona State University, Tempe AZ-85282, USA. Email: Christina.Birkel@asu.edu*
[c.] *Faculty of Physics and Center for Nanointegration Duisburg-Essen, University of Duisburg-Essen, Germany*
[d.] *Department of Chemistry, University College London, 20 Gordon Street, London, WC1H 0AJ, UK*
[e.] *Deutsches Elektronen-Synchrotron DESY, Notkestraße 85, 22607 Hamburg Germany*

Corresponding author: Christina S. Birkel, christina.birkel@asu.edu

The research in MAX phases is mainly concentrated on the investigation of carbides rather than nitrides (currently >150 carbides and only <15 nitrides) that are predominantly synthesized by conventional solid-state techniques. This is not surprising since the preparation of nitrides and carbonitrides is more demanding due to the high stability and low diffusion rate of nitrogen-containing compounds. This leads to several drawbacks concerning potential variations in chemical composition of the MAX phases as well as control of morphology, two aspects that directly affect the resulting materials properties. Here, we report how alternative solid-state hybrid techniques solve these limitations by combining conventional techniques with non-conventional precursor synthesis methods, such as the "urea-glass" sol-gel or liquid ammonia method. We demonstrate the synthesis and morphology control within the V-Ga-C-N system by preparing the MAX phase carbide, the nitride – the latter in the form of bulkier and more defined smaller particle structures – as well as a hitherto unknown carbonitride $V_2GaC_{1-x}N_x$ MAX phase. This shows the versatility of hybrid methods starting for example from wet-chemically obtained precursors that already contain all of the ingredients needed for carbonitride formation. All products are characterized in detail by X-ray powder diffraction, electron microscopy and electron and X-ray photoelectron spectroscopies in order to confirm their structure and morphology and to detect subtle differences between the different chemical compositions.

Introduction

One outstanding class of materials amongst transition metal carbides and nitrides are the so-called MAX phases. They are layered ternary compounds with hexagonal structure that are particularly fascinating due to their exceptional properties such as the unique combination of both metallic and ceramic characteristics[1], their complex magnetic behavior (if they contain Cr and Mn)[2], and their role to serve as precursors for a relatively new class of two-dimensional materials, the MXenes.[3]
The first MAX phase related report dates back to 1960 when Kudielka *et al.* synthesized carbosulfides of titanium and zirconium.[4] Further fundamental investigations were conducted in the following years by Jeitschko *et al.* who synthesized numerous members of a family they called H-phases.[5–7] However, until the 1990s, no particular attention was paid to this class of layered materials until Barsoum *et al.*[8] laid the foundation for the consistently growing field of what is now known as MAX phases.
The general chemical formula of MAX phases is $M_{n+1}AX_n$ (n = 1, 2, 3 (4,5)), where *M* is an early transition metal, *A* is a main group element mostly of groups 13 and 14, and *X* is carbon and/or nitrogen. They crystallize in space group $P6_3/mmc$ with edge-sharing M_6X octahedra interleaved with layers of *A* atoms.[1] Currently, more than 150 MAX phases are known,[9] which includes all known solid-solutions demonstrating their enormous chemical diversity. Amongst all MAX phases, only less than 15 are nitrides and carbonitrides (C and N on the *X* position) are even more scarce: Only a few reports on the quaternary Ti-Al-C-N system have been published.[10–13]
A variety of ternary V-containing MAX phases, such as aluminum,[5,14] germanium[6] and zinc-based phases,[15] respectively, as well as different solid-solution phases are known.[16,17] In this publication we turn our focus to the scarcely explored system of V – Ga – C – N . Both parent compounds V_2GaC and V_2GaN were initially synthesized by Jeitschko and co-workers in 1963.[5,7] For the nitride, up to now, despite successful synthesis, no experimental data are available.[7] The carbide V_2GaC has also hardly been described in the literature. Only its discovery amongst other "H"-phases, including experimental information on its synthesis has been reported.[5] Besides, both parent compounds were investigated by theory.[18,19]
The preparation of bulk MAX phases is traditionally conducted by conventional high-temperature solid-state techniques such as pressureless sintering,[20,21] arc melting and annealing,[22] or hot isostatic pressing.[23,24] Although these methods work well for the synthesis of a plethora of different MAX phases, they exhibit several drawbacks concerning energy efficiency, control of morphology, as well as process/reaction time.[25,26] Some of our recent works have already shown alternative approaches to face these drawbacks by applying methods such as microwave heating,[27,28] spark plasma sintering,[14] and a citrate-based sol-gel

method.[29] So far, we have mainly used these methods to produce known carbide phases.

The overwhelming predominance of carbide MAX phases by a factor of ten (>150 carbides and <15 nitrides) can be related to different challenges that occur during the synthesis of nitrides, such as the gaseous physical state of nitrogen under normal conditions, or its high bonding energy which is an inhibiting factor for a direct nitridation.[30] This in turn requires the use of binary precursors that must fulfil MAX phase stoichiometry. For the synthesis of the latter, several non-conventional methods have been developed and applied over the recent years.[31–33] One popular example is the so-called "urea glass-route", a sol-gel method established by Giordano and Antonietti *et al.* in 2008,[31] which easily enables the synthesis of nanoparticular carbides and nitrides by adjusting the urea amount, as a gel-forming agent. However, urea also causes carbon as an ingredient leading to carbonitride products because working in a carbon-free reaction mixture is not given in this case.[34] An elegant way to bypass carbon is to use liquid ammonia as a solvent and nitrogen source. It has the unique property to dissolve alkaline and alkaline earth metals into metal cations and solvated electrons.[35,36] The resulting solutions provide a high reduction potential that can be beneficially used in the synthesis of nanoparticular binary nitrides.[33,37–39]

Here, we demonstrate that the different synthesis techniques – solid-state, sol-gel and liquid ammonia based – can be specifically used for the preparation of the carbide, carbonitride and nitride MAX phases V_2GaC, $V_2GaC_{1-x}N_x$, and V_2GaN. While the carbide phase is prepared by a conventional one-step high-temperature solid-state reaction between elemental precursors, the (carbo)nitride MAX phases are prepared by a two-step process from binary (ternary) and nanoparticular precursors (VN and $VC_{1-x}N_x$) that are then reacted into the target MAX phases by a conventional annealing procedure.

Thus, by the flexible combination of different synthesis approaches and precursor mixtures, these hybrid methods extend the compositional space of accessible MAX phases. Beside the synthesis of the known carbide and nitride phases, V_2GaC and V_2GaN, our approach also represents an alternative way for the preparation of a hitherto unknown carbonitride MAX phase ($V_2GaC_{1-x}N_x$). Carbon and nitrogen on X sites within the MAX phase structure is proven by X-ray powder diffraction, electron energy loss spectroscopy, and X-ray photoelectron spectroscopy. Electron microscopies further show different morphologies depending on the synthesis routes.

Experimental section

In this work, we present four different types of samples in detail as illustrated in Figure 1: V_2GaC, $V_2GaC_{1-x}N_x$, and two V_2GaN phases, prepared by two different methods. In addition, we will briefly present results on a carbonitride prepared with a modified precursor ratio to introduce the idea that the C/N ratio can be controlled. The respective experimental conditions and procedures are described below, and further details are given in the SI (Tables SI-1 and SI-2).

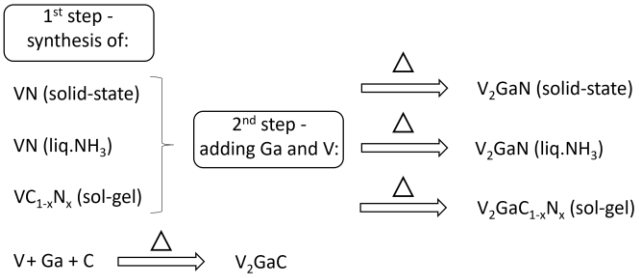

Figure 1: Schematic summary of the discussed V-based MAX phases samples, including the used precursors and synthesis methods.

We chose this set of samples because (i) it demonstrates a new synthesis route to access the nitride MAX phase V_2GaN involving carbon-free nitride precursor particles obtained from liquid ammonia, (ii) it shows that different morphologies of the nitride MAX phase can be obtained depending on the synthesis technique of the VN precursor, and (iii) it enables the synthesis of a hitherto unknown carbonitride $V_2GaC_{1-x}N_x$ for the first time.

Step 1: VN and $VC_{1-x}N_x$ precursor synthesis

(i) $VC_{1-x}N_x$ (sol-gel): Following the method by Giordano and Antonietti *et al.*[34], 0.6 ml (1.10 g, 6.32 mmol) of $VOCl_3$ (Sigma Aldrich, 99 %) were dissolved in ~3 ml ethanol under the release of HCl gas (inside a fume hood). The solution was stirred for 15 min and heated to 50 °C where 1.14 g (18.96 mmol) urea (Sigma Aldrich, >99 %) as gelation agent was added. The resulting homogeneous and highly viscous brownish gel was then transferred into an alumina crucible and annealed inside a horizontal tube furnace (Carbolite) at 850 °C (heating rate 2 °C/min) for eight hours under a continuous flow of nitrogen.

(ii) VN (liquid ammonia): Due to the high sensitivity of oxygen and water impurities in this synthesis technique, all glassware was heated under vacuum and purged with argon prior to synthesis. According to Zieschang *et al.*,[40] 2.97 g (18.90 mmol) of VCl_3 (Sigma Aldrich, >99 %) were weighed into a two-neck Schlenk flask equipped with a glass-coated magnetic stirrer in an argon-filled glovebox. Subsequently, ~60 ml of predried liquid ammonia (Praxair, UHP) were distilled into the two-neck Schlenk flask before 3.5 eq. sodium (1.51 g, 65.40 mmol) (Alfa Aesar, >99 %) were added under flowing argon. The suspension immediately turned black and was stirred for one hour at – 77 °C using an isopropanol-dry ice cooling bath. To remove remaining ammonia residues after completion of the reaction, the suspension was allowed to warm up to room temperature overnight. The obtained greyish powder was then annealed inside a vertical tube furnace (Carbolite) under vacuum following a defined temperature program (Table SI-2). To remove the side phase NaCl, the product was washed multiple times with 20 ml of predried methanol (molecular sieves 3 Å). The resulting finely dispersed black powder was stored inside an argon-filled glovebox.

(iii) VN (solid-state): 0.5 g (9.82 mmol) vanadium powder (Alfa Aesar, ~325 mesh, 99.5 %) were weighed into an alumina crucible in an argon-filled glovebox. Afterwards, the crucible was transferred into a horizontal tube furnace (Carbolite) and annealed for eight hours at 1250 °C (heating rate 5 °C/min) under a continuous flow of nitrogen.

Step 2: MAX phase synthesis

As illustrated in the scheme in Figure 1, V_2GaC is prepared by exclusively using elemental precursors, such as vanadium, gallium, and carbon in a solid-state reaction according to the following reaction equation:

$$2\ V + Ga + C \rightarrow V_2GaC$$

All syntheses of the (carbo)nitride MAX phases encompass two steps: In a first step, vanadium carbonitride and nitride precursors were prepared by different techniques, namely solid-state and liquid ammonia leading to nitrides, and "urea-glass" sol-gel leading to a carbonitride (details below). In the second step, the precursors (VN and $VC_{1-x}N_x$) were reacted with additional vanadium and gallium to ensure the target 2:1:1 stoichiometry according to the following reaction equations:

$$VC_{1-x}N_x + V + Ga \rightarrow V_2GaC_{1-x}N_x$$
$$VN + V + Ga \rightarrow V_2GaN$$

A typical synthesis involves mixing of the precursors based on 0.5 g (2.25 mmol) of the desired MAX phase. A detailed summary of the used amounts can be found in the SI (Table SI-1). Briefly, gallium flakes (Alfa Aesar, >99 %) were cut under atmospheric conditions and subsequently transferred into an argon-filled glovebox. A small excess of gallium was used to account for the slight gallium loss during reaction. Inside the glovebox, vanadium powder (Alfa Aesar, ~325 mesh, 99.5 %), the vanadium (carbo)nitride prepared in step 1 (see above), or carbon (Alfa Aesar, APS 2-15 micron, 99.999 %) were weighed and thoroughly homogenized using an agate mortar. Afterwards, the powder mixture was loosely mixed with the gallium flakes and pressed into a dense pellet (*d* = 10 mm, 3t, 30 s). All pellets were then annealed inside a horizontal tube furnace (Carbolite) following a defined temperature program (Table SI-2) under the exclusion of oxygen.

Characterization techniques

X-ray powder diffraction data were obtained using a D2 Phaser diffractometer (Bruker) with Cu-$K_{\alpha1}$ (λ = 1.540596 Å) and Cu-$K_{\alpha2}$ (1.544493 Å) in Bragg-Brentano geometry at room temperature. Prior to measurements, all samples were finely ground using an agate mortar and deposited on a low-background silicon specimen holder (Bruker). Rietveld refinements of the XRD data were conducted using DIFFRAC.TOPAS (Bruker). To maximize the accuracy of the lattice parameters, LaB_6 was used as an internal standard for all MAX phase samples (Figure SI-2).
SEM images were taken at the FEG XL30 (FEI) choosing acceleration voltages of 10-30 kV. The EDX data was collected with the XL-30 (EDAX) detector.
TEM samples were prepared by ultrasound-assisted dispersing the MAX phase powder in ethanol for 2 h and drop casting 3 µL on a Cu grid covered with a lacey carbon film. HRTEM images were acquired with a JEOL JEM-2200FS C_s-corrected transmission electron microscope at an acceleration voltage of 200 kV using a 2k x 2k GATAN UltraScan®1000XP CCD camera.

The electron energy loss spectroscopy (EELS) spectra were recorded in imaging mode. The core edges were extracted from the background signal using a power law. Both soft and hard X-ray photoelectron spectroscopy (SXPS and HAXPES) were used to characterize the chemical environments and oxidation states within the samples. SXPS data were recorded on a Thermo Scientific K-Alpha+ X-ray Photoelectron Spectrometer (XPS) system using monochromated, micro-focused Al-K_α X-ray radiation (*hv* = 1.4867 keV, further referred to as 1.5 keV for simplicity) and a 180° double-focusing hemispherical analyzer with a two-dimensional detector. The X-ray source was operated at 6 mA emission current and 12 kV anode bias. Data was collected using a 400 µm X-ray spot and a pass energy of 200 eV for survey and 20 eV for core level spectra. A flooding electron gun was used to minimize sample charging. HAXPES data were collected at beamline P22 at PETRA III, German Electron Synchrotron DESY in Hamburg, Germany.[41] A photon energy of 6.0054 keV (further referred to as 6 keV for simplicity) were used for all experiments, with the energy selected using a Si (111) double crystal monochromator and a Si (333) post-monochromator. All measurements were conducted in grazing incidence geometry (5°). A Phoibos 225HV analyzer (SPECS, Berlin, Germany) was used with the small area lens mode and a slit size of 3 mm. Spectra were collected using a pass energy of 30 eV. The total energy resolution in this setup was determined to be 242 meV 16/84% Fermi edge (E_F) width of a polycrystalline gold foil.

Results and Discussion

All nitride and carbonitride precursors are single-phase (Figure SI-1). For VN, the particles obtained from liquid ammonia show broader peaks in their XRD data, which indicates reduced crystallite sizes in comparison to the solid-state prepared ones with sharper peaks. The sol-gel derived carbonitride precursor also delivers broad peaks which is expected as a result of the wet chemical preparation. Indeed, crystallite sizes obtained from Scherrer broadening during Rietveld refinement range from an average of 30 nm (NH_3) to an average of 140 nm (sol-gel), see also Table SI-3.
The Rietveld refinements of the X-ray powder diffraction data of all target MAX phase samples are shown in Figure 2 which also includes the refined lattice parameters. Here, the structural models of V_2GaC[19] and side phases (VN[42]/($VC_{1-x}N_x$,) V_2O_3[43]) were fitted (orange line) to the diffraction data (black dots). To increase the accuracy of the calculated lattice parameters, LaB_6

was used as an internal standard (Figure SI-2). The full sets of results from the Rietveld refinements, including the phase fractions, are summarized in Tables SI-4-9). In all samples, the MAX phase forms the main phase with weight percentages up to 95 wt-% (V_2GaN). The observed oxide impurities in the liquid ammonia derived sample can be explained by oxygen impurities occurring during the very sensitive precursor synthesis. The powder XRD data of all samples show an absence of the (002) peak. This has also been observed in previous works of our group, focused on Ga-based phases.[29,44] However, its origin still has to be elucidated.

The lattice parameters of the nearly phase pure carbide phase V_2GaC are in good agreement with those reported in the literature.[19] In comparison, the *a*-lattice parameter of the conventionally synthesized nitride phase V_2GaN is noticeably smaller, while the *c*-parameter exhibits a larger value. Despite the increase of the latter, the overall cell volume shrinks by roughly 1 Å^3 to V = 94.37(8) Å^3 going from the carbide to the nitride. Considering the reported experimental lattice parameters[1] (a = 3.00 Å, c = 13.3 Å) for V_2GaN that lead to a cell volume of ~V = 103.7 Å^3, this shows a discrepancy between our experimental values for V_2GaN compared to the literature. Nonetheless, the calculated values of Bouhemadou *et al.*[18], as well as the smaller atomic radius of nitrogen compared to carbon, support our finding with a lower value in volume of the nitride. Furthermore, the cell volume (V = 94.67(2) Å^3) of our second V_2GaN sample (the one prepared from the liquid ammonia derived VN) confirms the smaller volume in comparison to the literature report. The carbonitride MAX phase prepared from the "urea-glass" precursors shows lattice parameters that fall in between those of the carbide and the nitride (closer to those of the carbide phase). This is an indication of C and N mixing on the *X* site of the MAX phase structure in $V_2GaC_{1-x}N_x$. This needs to be validated by further techniques (see below).

In order to confirm the feasibility of the sol-gel based synthesis approach, another exemplary $V_2GaC_{1-x}N_x$ phase was synthesized using a $VC_{1-x}N_x$ precursor prepared with a higher urea amount (8 eq. urea, see SI).

Beside the lattice parameter determination, *ex-situ* X-ray powder data (Figure SI-4) were used to elucidate the formation mechanism of the hitherto unknown carbonitride MAX phase, which can be described as follows. First, the elemental precursors vanadium and gallium form an intermetallic vanadium-gallium species (Ga_5V_2) at moderate temperatures, which further reacts either with VN or carbon at higher temperatures towards the desired MAX phase. Electron micrographs (Figure 3) show the morphology of the different MAX phase samples. They reveal the opportunity to influence the size, shape and microstructure of the target phases by applying the above-described hybrid synthesis methods.

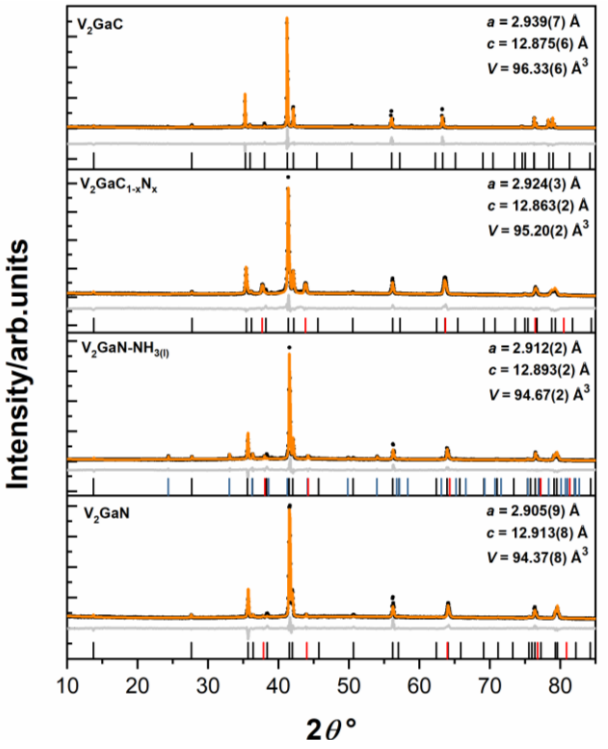

Figure 2: Results of the Rietveld refinements (orange lines) and residuum curves (grey) of the X-ray powder diffraction data (black dots) of the nitride, carbonitride, and carbide phases in the 211 V-Ga-C-N system. The refinements were conducted based on structural models of V_2GaC,[19] (black) VN[42] (red), and V_2O_3[43] (blue). The products are ordered according to increasing cell volumes. A full summary of the Rietveld data can be found in the SI.

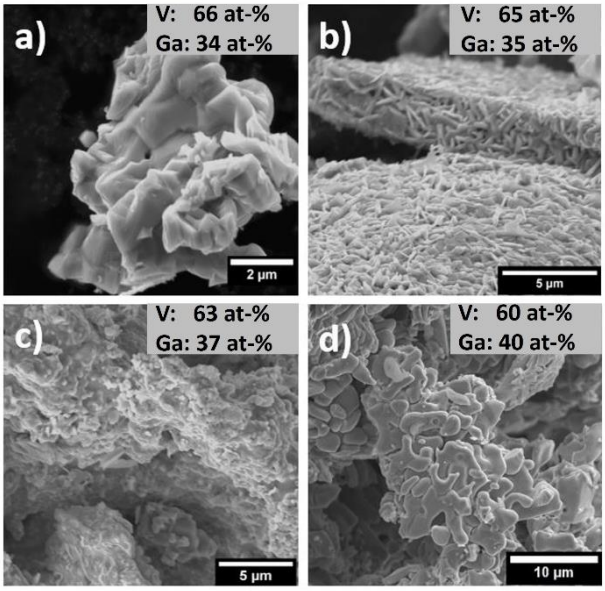

Figure 3: SEM micrographs of V_2GaC (a), $V_2GaC_{1-x}N_x$ (b), V_2GaN-$NH_{3(l)}$ (c), and V_2GaN (d), showing the various morphologies of the samples. The elemental compositions included in the micrographs were determined using EDX measurements (Tables SI-10-14).

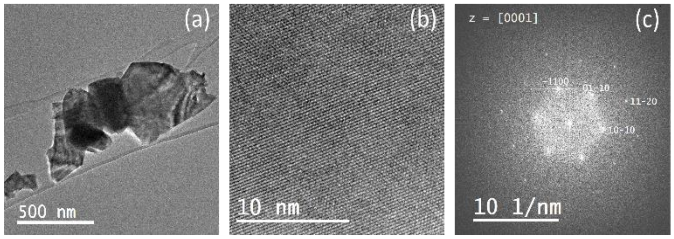

Figure 4: TEM (a) and HRTEM image (b) of $V_2GaC_{1-x}N_x$ MAX phase particles showing a typical morphology (a) and the MAX phase typical layered structure (b). The FFT in (c) allows to index the orientation which viewed along [0001].

While the morphology of the conventionally synthesized pure carbide V_2GaC is mainly dominated by the characteristic anisotropic MAX phase layered structure (Figure 3a), the sol-gel derived samples (Figure 3b) additionally exhibit a covered surface with needle-like structures (see also Figure SI-10 for the carbonitride sample prepared with 8 eq. urea). On the other hand, the conventionally synthesized pure nitride V_2GaN (Figure 3d) shows coarse and flake-like structures, whereas the liq. ammonia derived V_2GaN (Figure 3c) reveals finer substructures and drop-like particles partially covering the surface. This is most likely due to the nanoparticular character of the VN-precursor, which simultaneously influences the thermal behavior of the resulting MAX phase. While the conventional solid-state approach showed best results at 1700 °C, the ammonia derived MAX phase already decomposed at 1400 °C (Figure SI-5). Especially the latter example impressively demonstrates that the choice of the precursor and the resulting morphology can have a tremendous effect on the materials properties. Despite small deviations in the 2:1 V/Ga ratio, the compositions of the MAX phases were confirmed using EDX measurements (Figure 3, Tables SI-10-14). The microstructure of $V_2GaC_{1-x}N_x$ was further studied by high-resolution transmission electron microscopy. Figure 4a shows anisotropic flake-like morphology of the synthesized particles, while the corresponding HRTEM image reveals a well-ordered layered structure typical for nanolaminated MAX phases (further TEM data in Figure SI-11).

Core-loss EELS spectra recorded in the region from 250 to 600 eV clearly indicate the presence of the C, N, and V edges at about 290 eV, 400 eV, and 510 eV, respectively (Figure 5). We note that the C-K edge signal is slightly different from the typical MAX phase C-K edge describing a slight broadening of the second peak (≈295 eV), while the N-K edge shows all the features earlier observed for N-based MAX phases (Figure 5, inset).[12,45] These findings evidence that for the $V_2GaC_{1-x}N_x$ MAX phase N atoms are less sensitive to the perturbation induced by solid solution effects as compared to C atoms. Focusing further on the C-K and N-K edges, we quantify the C and N content, which is in average 45 at-% and 55 at-%, respectively. In this way, a sum formula can be formulated that approximately corresponds to a 0.5/0.5 ratio of carbon and nitrogen. Based on the determined C/N ratio by core-loss EELS spectra, a conventional solid-state approach using VN (solid state), carbon, vanadium, and gallium was conducted. When applying the same reaction conditions as in the sol-gel based approach, the X-ray powder diffraction data of the resulting product show the simultaneous presence of both, the parent phases V_2GaN and V_2GaC, and no clear evidence for a formation of the desired carbonitride phase (Figure SI-6). Only at 1100 °C a formation of $V_2GaC_{1-x}N_x$ can be realized, however, with a higher amount of side phase impurities (Figure SI-7, Table SI-15). These findings further support that the sol-gel based synthesis approach is a valuable option to extend the compositional space of MAX phases in terms of carbonitrides in combination with lower synthesis temperatures. Initial exploration of the samples using X-ray photoelectron spectroscopy was performed using a standard Al-K_α soft X-ray source. Whilst this provided good data for most of the core levels, the Ga LMM Auger series overlaps significantly with several essential core level spectra in this system, including N 1*s* and V 2*p*, making analysis and interpretation impossible (see Supplementary Information for the SXPS survey and core state spectra).

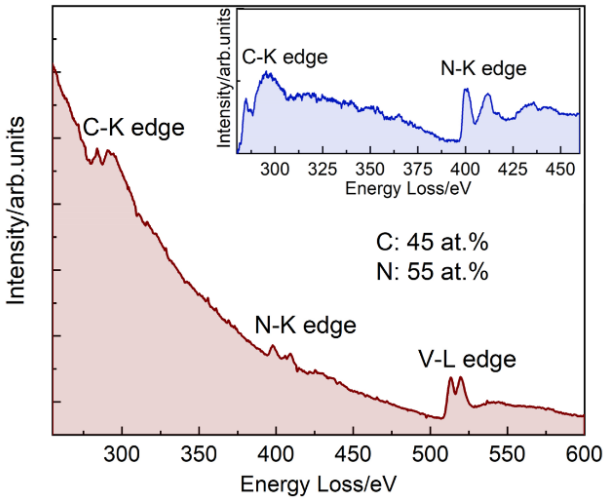

Figure 5: EELS spectra of C-K, N-K, and V-$L_{2,3}$ edges of a representative region of a $V_2GaC_{1-x}N_x$ particle and C and N composition as derived from elemental quantification of C-K and N-K edges EELS spectra (b, inset).

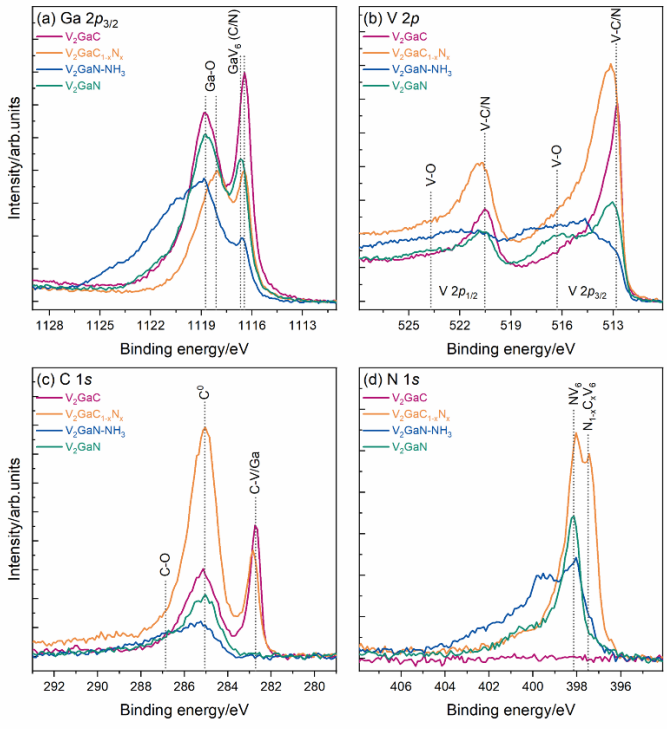

Figure 6: HAXPES data of all samples in the 211-V-Ga-C-N system, including (a) Ga $2p_{3/2}$, (b) V 2*p*, (c) C 1*s* and (d) N 1*s* core levels. All spectra were collected at hv = 6 keV.

Whilst core lines appear at the same binding energy in photoelectron spectra, independent of the excitation energy, Auger lines appear at specific kinetic energy. Changing the excitation energy used in a photoemission experiment will consequently move Auger lines relative to photoelectron lines. Therefore, HAXPES can be used to obtain spectra, which do not show any Auger contributions within the spectral range of interest (see Supplementary Information for HAXPES survey spectra).[46] Figure 6 shows the four main HAXPES core level spectra of all samples in the 211-V-Ga-C-N system. The Ga $2p_{3/2}$ core level (Figure 6(a)) shows sharp features at low binding energy (BE) from Ga in all investigated samples. Subtle differences in BE (Δ = 0.23 eV) are observed, with the pure carbide being the lowest in BE and the pure nitride being the highest in BE. In addition, all samples show contributions from oxidized environments, with clear differences between the pure carbide, nitride and the carbonitride. Whilst the SXPS spectra shown in the Supplementary Information (Figure SI-8) are dominated by the surface oxide layer, this contribution is lower in HAXPES due to the increased probing depth. As all samples were handled in air, it is expected that the surface of the samples will be partially oxidized. The spectral shape of the liquid ammonia-based sample is clearly different from the other samples. We discuss the data for this sample separately below. The V 2*p* core level for all other samples (Figure 6 (b)) shows the typical doublet, with the $2p_{1/2}$ state considerably broadened by Coster-Kronig effects.[47] V_2GaC exhibits the sharpest, asymmetric $2p_{3/2}$ feature at 512.8 eV. The spectra for V_2GaN and the mixed phase are broader and shifted to higher BE. In addition, all N-containing samples reveal clear contributions of oxidized states at higher BE. The C-1*s* spectra (Figure 6(c)) clearly distinguish between the pure nitride samples, and the carbide and carbonitride phases. Only the latter phases have a clear low BE feature at 282.7 eV. All samples exhibit varying contributions from adventitious carbon (C^0) from exposure to air as well as small amounts of C-O environments. Finally, in the N 1*s* spectra (Figure 6 (d)) V_2GaN shows one clear feature at 398.2 eV for the NV_6 environments A lower BE feature (397.5 eV) is found for the $V_2GaC_{1-x}N_x$ sample, commensurate with mixed $N_{1-x}C_xV_6$ environments. No nitrogen is detected in the carbide sample.

The liquid ammonia-based sample clearly differs across all HAXPES spectra. This is due to partial charging of the surface overlayer of this sample. In both SXPS and HAXPES, the V_2GaN-$NH_{3(l)}$ sample shows the highest degree of a surface overlayer as well as the presence of vanadium oxide consistent with the XRD analysis. The SXPS data for this sample (see Figure SI-9), where charge compensation could be used, shows a Ga $2p_{3/2}$ line shape comparable to that of the V_2GaN sample. Furthermore, the lower BE features across its HAXPES spectra match those of V_2GaN environments observed for the sample prepared through the solid-state route.

Conclusion

By combining non-conventional precursor synthesis methods, such as the sol-gel "urea-glass" and liquid ammonia method with conventional solid-state preparation techniques, we demonstrated an alternative synthesis approach for the 211-V-Ga-C-N MAX phase system. Beside the synthesis of the pure carbide and nitride phases, the sol-gel based method represented a valuable option to synthesize a hitherto unknown carbonitride phase $V_2GaC_{1-x}N_x$. The mixed C/N nature within the M_6X octahedra of the new carbonitride phase was proven by means of X-ray powder diffraction, electron energy loss spectroscopy and X-ray photoelectron spectroscopy, respectively. On the other hand, the liquid-ammonia based approach provides a new way to access the hardly investigated research field of nitride MAX phases, whose syntheses are challenging due to inhibiting factors occurring during nitride synthesis. Additionally, SEM micrographs revealed the potential of hybrid solid-state techniques to specifically influence the morphology of the obtained MAX phases depending on the synthesis process. In terms of phase purity of the products, both synthesis approaches will be further optimized to suppress the present side phases in future studies. However, overall, the findings of this work underline the beneficial aspect of non-conventional approaches to not only extend the phase variety, but also to be a tool for targeted solid-state product design, that may be extended to further non-oxide compounds, even beyond MAX phases.

Associated Content

Supporting Information Available:

The supporting information includes a detailed description of the reaction parameters, as well as the full sets of results of all Rietveld refinements. Besides, XRD data are available that further clarify the reaction mechanism of the carbonitride phase $V_2GaC_{1-x}N_x$ and the temperature stability of the liq. NH_3 derived MAX phase sample. Furthermore, a summary of the EDX measurements, further SEM/TEM micrographs, and additional SXPS and HAXPES data can be found.

This information is available free of charge at the website: **:** https://urldefense.com/v3/__http://pubs.acs.org__;!!IKRxdwAv5BmarQ!ezEADNgx9MskQ-kJ7GykQRQWNh-TfM8hrswexm2rTwdi8CP7qiGl8dm5qFzvy7ECOn1K-jRnSBiKU4AY6qVMx0bvj8jHL44h1A$

Author Contributions

N.K. and A.R. conducted the experiments and X-ray diffraction data and wrote the manuscript, N.K. conducted the SEM study and evaluated the XRD and SEM data. H.P. conducted the TEM/EELS study, evaluated the data and wrote the manuscript, A.-M.Z. and B.A. assisted with the design of the ammonia plant and edited the manuscript, C.K., C.S. and A.R. conducted the XPS study, evaluated the data and wrote the manuscript, U.W. and C.B. wrote the manuscript, C.B. provided the research question and coordinated the contributions.

Conflicts of interest

There are no conflicts to declare.

Acknowledgements

This work has been supported by the Deutsche Forschungsgemeinschaft (DFG) within CRC/TRR 270, projects B03 and B02 (Project-ID 405553726). Further support by the Deutsche Forschungsgemeinschaft has been provided through a Walter Benjamin Fellowship (Project-ID: 456639820). Support by the Interdisciplinary Center for Analytics on the Nanoscale (ICAN) of the University of Duisburg-Essen (DFG RIsources reference: RI_00313), a DFG-funded core facility (Project Nos. 233512597 and 324659309), is gratefully acknowledged. AR acknowledges support from the Analytical Chemistry Trust Fund for her CAMS-UK fellowship. CK acknowledges support from the Department of Chemistry, UCL. We acknowledge DESY (Hamburg, Germany), a member of the Helmholtz Association HGF, for the provision of experimental facilities. Parts of this research were carried out at PETRA III using beamline P22. Beamtime was allocated for proposal I-20210139EC."

Notes and references

(1) Barsoum, M. W. The M_{n+1} AX_n Phases : A New Class of Solids. *Prog. Solid State Chem.* **2000**, *28*, 201–281.

(2) Ingason, A. S.; Mockute, A.; Dahlqvist, M.; Magnus, F.; Olafsson, S.; Arnalds, U. B.; Alling, B.; Abrikosov, I. A.; Hjörvarsson, B.; Persson, P. O. Å.; Rosen, J. Magnetic Self-Organized Atomic Laminate from First Principles and Thin Film Synthesis. *Phys. Rev. Lett.* **2013**, *110* (19), 2–6.

(3) Naguib, M.; Mashtalir, O.; Carle, J.; Presser, V.; Lu, J.; Hultman, L.; Gogotsi, Y.; Barsoum, M. W. Two-Dimensional Transition Metal Carbides. *ACS Nano* **2012**, *6* (2), 1322–1331.

(4) Kudielka, H.; Rohde, H. Strukturuntersuchungen an Carbosulfiden von Titan Und Zirkon. *Zeitschrift für Krist.* **1960**, *114*, 447–456.

(5) Jeitschko, W.; Nowotny, H.; Benesovsky, F. Kohlenstoffhaltige Ternäre Verbindungen (H-Phase). *Monatshefte für Chemie* **1963**, *94* (4), 672–676.

(6) Jeitschko, W.; Nowotny, H.; Benesovsky, F. Kohlenstoffhaltige Ternäre Verbindungen (V-Ge-C, Nb-Ga-C, Ta-Ga-C, Ta-Ge-C, Cr-Ga-C Und Cr-Ge-C). *Monatshefte für Chemie* **1963**, *94* (5), 844–850.

(7) Jeitschko, W.; Nowotny, H.; Benesovsky, F. Ternäre Carbide Und Nitride in Systemen: Übergangsmetall-Metametall-Kohlenstoff (Stickstoff). *Monatshefte für Chemie* **1964**, *95* (1), 156–157.

(8) Barsoum, M. W.; El-Raghy, T. Synthesis and Characterization of a Remarkable Ceramic: Ti_3SiC_2. *Journal of the American Ceramic Society*. **1996**, 1953–1956.

(9) Sokol, M.; Natu, V.; Kota, S.; Barsoum, M. W. On the Chemical Diversity of the MAX Phases. *Trends Chem.* **2019**, *1* (2), 210–223.

(10) Cabioc'h, T.; Eklund, P.; Mauchamp, V.; Jaouen, M. Structural Investigation of Substoichiometry and Solid Solution Effects in $Ti_2Al(C_x,N_{1-x})_y$ Compounds. *J. Eur. Ceram. Soc.* **2012**, *32* (8), 1803–1811.

(11) Pietzka, M. A.; Schuster, J. C. Phase Equilibria in the Quarternary System Ti-Al-C-N. *J. Am. Ceram. Soc.* **1996**, *79* (9), 2321–2330.

(12) Yu, W.; Mauchamp, V.; Cabioc'H, T.; Magne, D.; Gence, L.; Piraux, L.; Gauthier-Brunet, V.; Dubois, S. Solid Solution Effects in the $Ti_2Al(C_xN_y)$ MAX Phases: Synthesis, Microstructure, Electronic Structure and Transport Properties. *Acta Mater.* **2014**, *80*, 421–434.

(13) Prikhna, T.; Cabioc'h, T.; Gawalek, W.; Ostash, O.; Litzkendorf, D.; Dub, S.; Loshak, M.; Sverdun, V.; Chartier, P.; Basyuk, T.; Moshchil, V.; Kozyrev, A.; Karpets, M.; Kovylaev, V.; Starostina, A.; Turkrvich, D. Study of the Thermal Stability and Mechanical Characteristics of MAX Phases of Ti-Al-C(N) System and Their Solid Solutions. *Adv. Sci. Technol.* **2014**, *89*, 123–128.

(14) Hamm, C. M.; Schäfer, T.; Zhang, H.; Birkel, C. S. Non-Conventional Synthesis of the 413 MAX Phase V_4AlC_3. *Ceram. Int.* **2016**, No. 23, 1397–1401.

(15) Li, M.; Lu, J.; Luo, K.; Li, Y.; Chang, K.; Chen, K.; Zhou, J.; Rosen, J.; Hultman, L.; Eklund, P.; Persson, P. O. Å.; Du, S.; Chai, Z.; Huang, Z.; Huang, Q. Element Replacement Approach by Reaction with Lewis Acidic Molten Salts to Synthesize Nanolaminated MAX Phases and MXenes. *J. Am. Chem. Soc.* **2019**, *141* (11), 4730–4737.

(16) Caspi, E. N.; Chartier, P.; Porcher, F.; Damay, F.; Cabioc'h, T. Ordering of (Cr,V) Layers in Nanolamellar $(Cr_{0.5}V_{0.5})_{n+1}AlC_n$ Compounds. *Mater. Res. Lett.* **2015**, *3* (2), 100–106.

(17) Zhou, Y.; Meng, F.; Zhang, J. New MAX-Phase Compounds in the V–Cr–Al–C System. *J. Am. Ceram. Soc.* **2008**, *91* (4), 1357–1360.

(18) Bouhemadou, A. Structural, Electronic and Elastic Properties of MAX Phases M_2GaN (M = Ti, V and Cr). *Solid State Sci.* **2009**, *11* (11), 1875–1881.

(19) Shein, I. R.; Ivanovskii, A. L. Structural, Elastic, Electronic Properties and Fermi Surface for Superconducting Mo_2GaC in Comparison with V_2GaC and Nb_2GaC from First Principles. *Phys. C Supercond.* **2010**, *470* (13–14), 533–537.

(20) Sato, K.; Mishra, M.; Hirano, H.; Hu, C.; Sakka, Y. Pressureless Sintering and Reaction Mechanisms of Ti_3SiC_2 Ceramics. *J. Am. Ceram. Soc.* **2014**, *97* (5), 1407–1412.

(21) Horlait, D.; Grasso, S.; Chroneos, A.; Lee, W. E. Attempts to Synthesise Quaternary MAX Phases $(Zr,M)_2AlC$ and $Zr_2(Al,A)C$ as a way to approach Zr_2AlC. *Mater. Res. Lett.* **2016**, *4* (3), 137–144.

(22) Arunajatesan, S.; Carim, A. H. Synthesis of Titanium Silicon Carbide. *J. Am. Ceram. Soc.* **1995**, *78* (3), 667–672.

(23) Dubois, S.; Cabioc'h, T.; Chartier, P.; Gauthier, V.; Jaouen, M. A New Ternary Nanolaminate Carbide: Ti_3SnC_2. *J. Am. Ceram. Soc.* **2007**, *90* (8), 2642–2644.

(24) Barsoum, M. W.; Salama, I.; El-Raghy, T.; Golczewski, J.; Porter, W. D.; Wang, H.; Seifert, H. J.; Aldinger, F. Thermal and Electrical Properties of Nb_2AlC, $(Ti,Nb)_2AlC$ and Ti_2AlC. *Metall. Mater. Trans. A Phys. Metall. Mater. Sci.* **2002**, *33* (9), 2775–2779.

(25) Siebert, J. P.; Hamm, C. M.; Birkel, C. S. Microwave Heating and Spark Plasma Sintering as Non-Conventional Synthesis Methods to Access Thermoelectric and Magnetic Materials. *Appl. Phys. Rev* **2019**, *6*, 41314.

(26) Groh, M. F.; Heise, M.; Kaiser, M.; Ruck, M. Sanfte Festkörperchemie. **2013**, 26–29.

(27) Hamm, C. M.; Bocarsly, J. D.; Seward, G.; Kramm, U. I.; Birkel, C. S. Non-Conventional Synthesis and Magnetic Properties of MAX Phases $(Cr/Mn)_2AlC$ and $(Cr/Fe)_2AlC$. *J. Mater. Chem. C* **2017**, *5* (23), 5700–5708.

(28) Hamm, C. M.; Dürrschnabel, M.; Molina-Luna, L.; Salikhov, R.; Spoddig, D.; Farle, M.; Wiedwald, U.; Birkel, C. S. Structural, Magnetic and Electrical Transport Properties of Non-Conventionally Prepared MAX Phases V_2AlC and $(V/Mn)_2AlC$. *Mater. Chem. Front.* **2018**, *2* (3), 483–490.

(29) Siebert, J. P.; Bischoff, L.; Lepple, M.; Zintler, A.; Molina-Luna, L.; Wiedwald, U.; Birkel, C. S. Sol-Gel Based Synthesis and Enhanced Processability of MAX Phase Cr_2GaC. *J. Mater. Chem. C* **2019**, *7* (20), 6034–6040.

(30) Greenaway, A. L.; Melamed, C. L.; Tellekamp, M. B.; Woods-Robinson, R.; Toberer, E. S.; Neilson, J. R.; Tamboli, A. C. Ternary Nitride Materials: Fundamentals and Emerging Device Applications. *Annu. Rev. Mater. Res.* **2020**, *51*, 1–28.

(31) Giordano, C.; Erpen, C.; Yao, W.; Antonietti, M. Synthesis of Mo and W Carbide and Nitride Nanoparticles via a Simple "Urea Glass" Route. *Nano Lett.* **2008**, *8* (12), 4659–4663.

(32) Kim, I.; Kumta, P. N. Hydrazide Sol–Gel Synthesis of Nanostructured Titanium Nitride: Precursor Chemistry and Phase Evolution. *J. Mater. Chem.* **2003**, *13* (8), 2028–2035.

(33) Zieschang, A.-M.; Seshadri, R.; Albert, B. Nanoscale Iron Nitride, ε-Fe_3N: Preparation from Liquid Ammonia and Magnetic Properties. *Chem. Mater.* **2017**, *29* (2), 621–628.

(34) Giordano, C.; Erpen, C.; Yao, W.; Milke, B.; Antonietti, M. Metal Nitride and Metal Carbide Nanoparticles by a Soft Urea Pathway. *Chem. Mater.* **2009**, *21* (21), 5136–5144.

(35) Fowles, G. W. A.; Nicholls, D. Inorganic Reactions in Liquid Ammonia. *Q. Rev. Chem. Soc.* **1962**, *16* (1), 19.

(36) Johnson, W. C.; Meyer, A. W. The Properties of Solutions of Metals in Liquid Ammonia. *Chem. Rev.* **1931**, *8* (2), 273–301.

(37) Zieschang, A. M.; Bocarsly, J. D.; Dürrschnabel, M.; Kleebe, H. J.; Seshadri, R.; Albert, B. Low-Temperature Synthesis and Magnetostructural Transition in Antiferromagnetic, Refractory Nanoparticles: Chromium Nitride, CrN. *Chem. Mater.* **2018**, *30* (5), 1610–1616.

(38) Yuan, B.; Yang, M.; Zhu, H. Titanium Nitride Nanopowders Produced via Sodium Reduction in Liquid Ammonia. *J. Mater. Chem. C* **2009**, *24*, 448–451.

(39) Han, Z.; Yang, M.; Zhu, H. Synthesis and Sintering of Aluminium Nitride Nano-Particles. *Mater. Res. Soc. Symp. Proc.* **2008**, *1040*, 134–139.

(40) Zieschang, A.-M. Nanopartikuläre 3d-Übergangsmetallnitride Aus Flüssigem Ammoniak, Dissertation, Technische Universität Darmstadt, 2019.

(41) Schlueter, C.; Gloskovskii, A.; Ederer, K.; Schostak, I.; Piec, S.; Sarkar, I.; Matveyev, Y.; Lömker, P.; Sing, M.; Claessen, R.; Wiemann, C.; Schneider, C. M.; Medjanik, K.; Schönhense, G.; Amann, P.; Nilsson, A.; Drube, W. The New Dedicated HAXPES Beamline P22 at PETRAIII. *AIP Conf. Proc.* **2019**, *2054* (January 2019).

(42) Hosoya, S.; Yamagishi, T.; Tokonami, M. Study of Electron State in Vanadium Nitride by Intensity Measurements of X-Ray Diffraction. *J. Phys. Soc. Japan* **1968**, *24* (2), 363–367.

(43) Rice, C. E.; Robinson, W. R. Structural Changes in the Solid Solution $(Ti_{1-x}V_x)_2O_3$ as x Varies from Zero to One. *J. Solid State Chem.* **1977**, *21* (2), 145–154.

(44) Siebert, J. P.; Mallett, S.; Juelsholt, M.; Pazniak, H.; Wiedwald, U.; Page De, K.; Birkel, C. S. Structure Determination and Magnetic Properties of the Mn-Doped MAX Phase Cr_2GaC. *J. Mater. Chem. Front* **2021**, *5*, 6082.

(45) Hug, G.; Jaouen, M.; Barsoum, M. W. X-Ray Absorption Spectroscopy, EELS, and Full-Potential Augmented Plane Wave Study of the Electronic Structure of Ti_2AlC, Ti_2AlN, Nb_2AlC, and $(Ti_{0.5}Nb_{0.5})_2AlC$. *Phys. Rev. B* **2005**, *71* (2), 24105.

(46) Kalha, C.; Fernando, N. K.; Bhatt, P.; Johansson, F. O. L.; Lindblad, A.; Rensmo, H.; Medina, L. Z.; Lindblad, R.; Siol, S.; Jeurgens, L. P. H.; Cancellieri, C.; Rossnagel, K.; Medjanik, K.; Schönhense, G.; Simon, M.; Gray, A. X.; Nemšák, S.; Lömker, P.; Schlueter, C.; Regoutz, A. Hard X-Ray Photoelectron Spectroscopy: A Snapshot of the State-of-the-Art in 2020. *J. Phys. Condens. Matter* **2021**, *33* (23), 233001.

(47) Nyholm, R.; Martensson, N.; Lebugle, A.; Axelsson, U. Auger and Coster-Kronig Broadening Effects in the 2p and 3p Photoelectron Spectra from the Metals ^{22}Ti-^{30}Zn. *J. Phys. F Met. Phys.* **1981**, *11* (8), 1727.

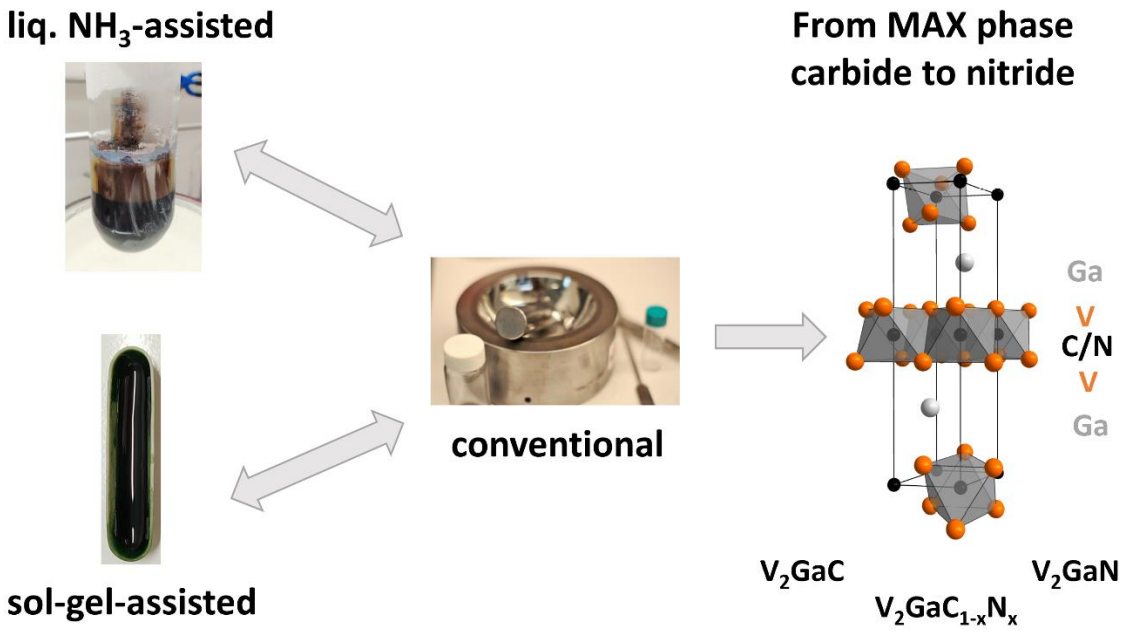

Utilizing diverse synthesis methods with solid-state or wet chemically derived precursors allows control over the chemical composition of a V-based MAX phase leading to a carbide, nitride as well as a hitherto unknown carbonitride phase. The morphology of the products is also affected by the synthesis of choice with wet chemical-based techniques leading to more defined/smaller particles than obtained by pure solid-state synthesis.